

デザイン・ガイド: TIDA-050022

# 100VIN 未満の DC/DC コンバータ向け電力段のリファレンス・デザイン



### 概要

このリファレンス・デザインでは、UCC27282 120V ハーフブリッジ MOSFET ドライバと CSD19531 100V パワー MOSFET をベースとして、高周波電力段の設計を実装します。このデザインは、高効率のスイッチと柔軟な  $V_{GS}$  動作範囲により、全体のゲート駆動損失および伝導損失を減らし、最高の効率を実現できます。この電力段のデザインは、テレコムのブリック電源モジュール、ソーラー・インバータ、DC モータ・ドライブなど、スペースの制約が厳しい多くのアプリケーションに広く適用可能です。

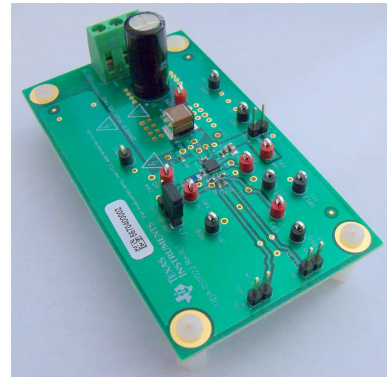
### リソース

<a href="#">TIDA-050022</a>	デザイン・フォルダ
<a href="#">UCC27282</a>	プロダクト・フォルダ
<a href="#">CSD19531</a>	プロダクト・フォルダ

[E2E™ エキスパートに質問](#)

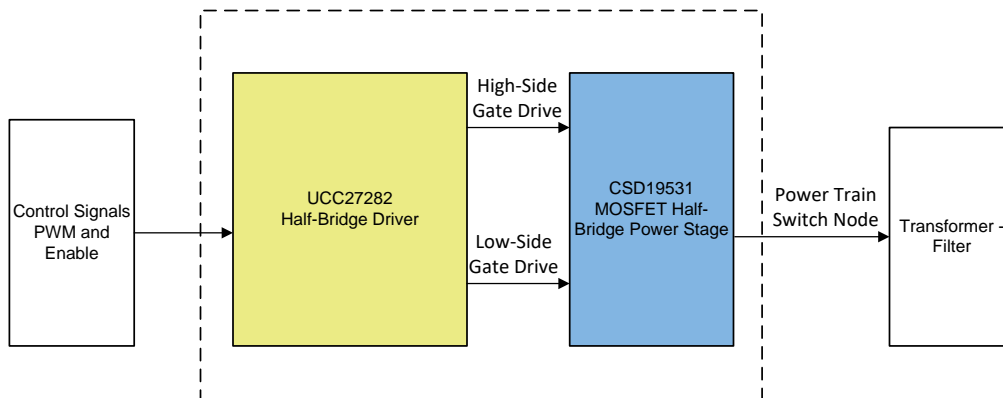
### 特長

- 小型の 100V 電力段設計で、最高 1MHz のスイッチング
- ハイサイドとローサイドに独立のパルス幅変調 (PWM) 入力があり、クロス導通保護を搭載
- 16ns の短い伝播遅延、遅延マッチングは標準値 1ns、最大値 7ns
- ドライバ VDD 動作範囲 6V~16V
- 負電圧能力によりノイズの大きな環境でも動作可能
- 小さなスタンバイ電流によるイネーブル



### アプリケーション

- テレコムのブリック電源モジュール
- ソーラー・マイクロ・インバータおよび電源最適化
- サーバーおよびネットワーク用電源
- DC モータ・ドライブ





使用許可、知的財産、その他免責事項は、最終ページにあるIMPORTANT NOTICE (重要な注意事項)をご参照くださいますようお願いいたします。

## 1 System Description

Telecom and datacom equipment capabilities keep increasing with demand for more processing power within a given size, or even size reduction as well. Increased capabilities of the equipment result in more demand from the power supplies. The power supplies in these systems must be optimized from a space utilization an efficiency standpoint. The complexity of control and interface is also increasing in telecom, datacom, and solar systems which make them more susceptible to noise and transients .

The half-bridge driver and power MOSFET power stage is used in a variety of DC/DC converter topologies including half-bridge, full bridge, synchronous buck, and full-bridge synchronous rectification. Solar micro inverters, solar optimizers and motor drive also use this power stage in many applications.

This reference design uses CSD19531 NexFET™ Si power MOSFETs and the UCC27282 120-V half-bridge driver to realize a power stage with high efficiency. The half-bridge driver allows two independent inputs for high-side and low-side gate drive and has cross conduction protection which turns off both gate drive signals in the event both inputs are high. The cross conduction protection does not have a fixed dead time so the controller can control precise timing of the turn on and turn off of the power MOSFETs.

This design can be applied to many high-efficiency applications such as telecom power modules, solar power, 48V server power, and industrial power supplies.

### 1.1 Key System Specifications

表 1. Key System Specifications

PARAMETER	TEST CONDITIONS	MIN	TYP	MAX	UNITS
<b>INPUT AND OUTPUT CHARACTERISTICS</b>					
Input and output voltage		0		100 <sup>(1)</sup>	V
Input and output current		0	4	8	A
Bias voltage		6	8	16	V
LI and HI Inputs to VGS Delay			15	30	ns
Delay Matching	LI/HI Complimentary		1	7	ns
<b>SYSTEM CHARACTERISTICS</b>					
Switching frequency		10	200	1000	kHz
Efficiency	$V_{IN} = 48\text{ V}, V_{OUT} = 24\text{ V}, I_{OUT} = 4\text{ A},$ $f_{SW} = 200, 300\text{ kHz}$	94	95	95.3	%

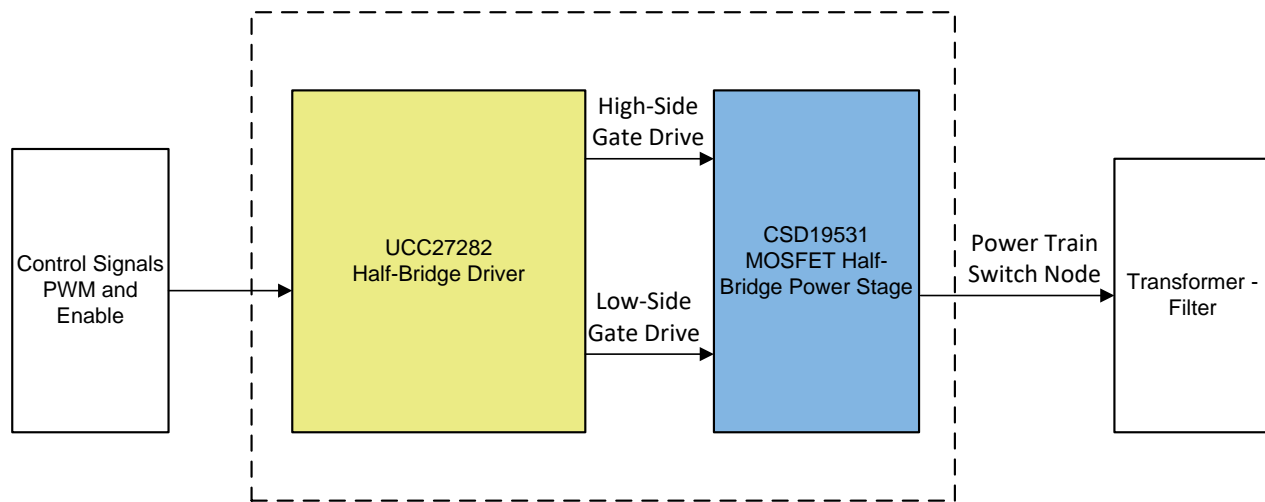
<sup>(1)</sup> HS voltage (MOSFET switch node) is limited to 100 V including overshoot. This may limit input voltage to a lower value.

## 2 System Overview

### 2.1 Block Diagram

Figure 1 shows the block diagram of this design. One half-bridge driver UCC27282 drives two MOSFETs in a half-bridge configuration. Two 100-V rated CSD19531 FETs are used as switching devices.

Figure 1. TIDA-050022 Block Diagram



### 2.2 Design Considerations

#### 2.2.1 FET Selection

The majority of 48 V input voltage telecom and datacom power module designs have gate driver bias voltage ( $V_{DD}/V_{CC}$ ) voltage in the 9 V to 10 V range using 100 V ( $V_{DS}$ ) rated power MOSFETs. The gate drive losses are reduced with lower gate drive voltage ( $V_{GS}$ ) and many MOSFET devices  $R_{DS(on)}$  versus  $V_{GS}$  curves indicate that there is little reduction in  $R_{DS(on)}$  beyond 8 V to 10V  $V_{GS}$ . One consideration of selecting the driver  $V_{DD}$  is the turn on UVLO threshold and including some margin for negative voltage transients on the bias supply. This may result in selecting the driver  $V_{DD}$  to be higher than the optimum gate drive and conduction loss operating point when using previous generation drivers.

The CSD10531 100V 5.3 m $\Omega$  MOSFET total gate charge, or  $Q_G$ , vs  $V_{GS}$  and the  $R_{DS(on)}$  vs  $V_{GS}$  can be viewed in the [CSD19531 data sheet](#). Although this MOSFET has an  $R_{DS(on)}$  specification with  $V_{GS} = 6$  V you can see that the  $R_{DS(on)}$  curve still has a noticeable declining  $R_{DS(on)}$  vs  $V_{GS}$  at 6 V. At  $V_{GS} = 8$  V the curve slope is much lower.

The gate drive losses for each driver output channel are dependent on  $V_{DD}$ , switching frequency ( $f_{SW}$ ), and MOSFET  $Q_G$  as shown in 式 1.

$$P_{GD} = V_{DD} \times f_{SW} \times Q_G \quad (1)$$

Another consideration for applications which will have body diode conduction during the switching transitions such as synchronous buck or synchronous rectification is the body diode  $t_{rr}$  and  $Q_{rr}$ . The body diode reverse recovery losses  $\Delta$  can exceed conduction loss  $\Delta$  even though the  $R_{DS(on)}$  is lower if the body diode reverse recovery time is longer. See 表 2 for parameter comparison of the CSD19531 MOSFET and CSD19533 MOSFET.

表 2. Parameter Comparison of Switching FETs

PARAMETER	CSD19531	CSD19533
Max $V_{DS}$ (V)	100	100
$R_{DS(on)}$ (m $\Omega$ ), $V_{GS}=10$ V	5.3	7.8
$R_{DS(on)}$ (m $\Omega$ ), $V_{GS}=6$ V	6.0	8.7
$Q_g$ (nC)	37	27
$t_{rr}$ (ns), Body Diode	147	62
$Q_{rr}$ (nC), Body Diode	226	163

## 2.2.2 Component Selection

### 2.2.2.1 Bootstrap and VDD Capacitor

The bootstrap capacitor must maintain the  $V_{HB-HS}$  voltage above the UVLO threshold for normal operation. To determine the minimum required bootstrap capacitance first calculate the maximum allowable drop across the bootstrap capacitor,  $\Delta V_{HB}$ , with 式 2.

$$\Delta V_{HB} = V_{DD} - V_{DH} - V_{HBL}$$

where

- $V_{DD}$  is the supply voltage of the gate driver device
- $V_{DH}$  is the bootstrap diode forward drop
- $V_{HBL}$  is the HB falling UVLO threshold ( $V_{HBR(max)} - V_{HBH}$ )

Many applications may target ripple voltage lower than the equation result, such as 0.5 V to 1 V ripple.

Determine the estimated charge per switching cycle from the bootstrap capacitor with 式 3.

$$Q_{TOTAL} = Q_G + I_{HBS} \times \left( \frac{D_{MAX}}{f_{SW}} \right)$$

where

- $Q_G$  is the total MOSFET gate charge
- $I_{HBS}$  is the HB to VSS leakage current
- $D_{Max}$  is the converter maximum duty cycle
- $I_{HB}$  is the HB quiescent current

Once the total charge is known the minimum bootstrap capacitance can be determined as follows in 式 4.

$$C_{BOOT(min)} = \frac{Q_{TOTAL}}{\Delta V_{HB}}$$

The bootstrap capacitor should be X7R or better dielectric with low inductance package(s). Also since the capacitance is reduced with DC bias, choose a capacitor with at least two times the expected maximum voltage in the application.

TI recommends the VDD capacitor value at least 10x the value of the bootstrap capacitance to minimize VDD ripple from charging the bootstrap capacitor. The VDD capacitor should also be X7R or better temperature stability dielectric. It is recommended to parallel a high frequency bypass capacitor in a small package size, 0402, and low value such as 1nF to filter high frequency noise with the VDD capacitor.

### 2.2.2.2 External Gate Resistor

In high frequency switching power supply applications where high-current gate drivers such as the UCC27282 are used, high current loops with parasitic inductances and parasitic capacitances can cause noise and ringing on the gate of power MOSFETs. Gate resistors are used often to damp this ringing and noise. There are also cases where gate resistance may be selected to address EMI and excessive switch node voltage spikes. It is good practice to make provisions for external gate resistors to allow addressing these possible issues.

Use the following equations to calculate the driver pullup and pulldown current.

The high-side driver pullup current can be determined with 式 5.

$$I_{OHH} = \frac{V_{DD} - V_{DH}}{R_{HOH} + R_{GATE} + R_{GFET(int)}}$$

where

- $I_{OHH}$  is the high-side peak pullup current
- $V_{DH}$  is the bootstrap diode forward drop
- $R_{HOH}$  is the gate driver internal high-side pullup resistance. Value can be calculated from test conditions ( $R_{HOH} = V_{HOH}/I_{HO}$ )
- $R_{GATE}$  is the external gate resistance between the driver output and MOSFET gate
- $R_{GFET(int)}$  is the MOSFET internal gate resistance in the MOSFET datasheet

(5)

The high-side driver sink current can be determined with 式 6.

$$I_{OLH} = \frac{V_{DD} - V_{DH}}{R_{HOL} + R_{GATE} + R_{GFET(int)}}$$

where

- $I_{OLH}$  is the high-side peak pullup current
- $R_{HOL}$  is the gate driver internal high-side pull-down resistance. Value can be calculated from test conditions ( $R_{HOL} = V_{HOL}/I_{HO}$ )

(6)

The low-side driver pullup current can be calculated with 式 7.

$$I_{OHL} = \frac{V_{DD}}{R_{LOH} + R_{GATE} + R_{GFET(int)}}$$

where

- $R_{LOH}$  is the gate driver low-side pullup resistance

(7)

The low side driver sink current can be determined with 式 8.

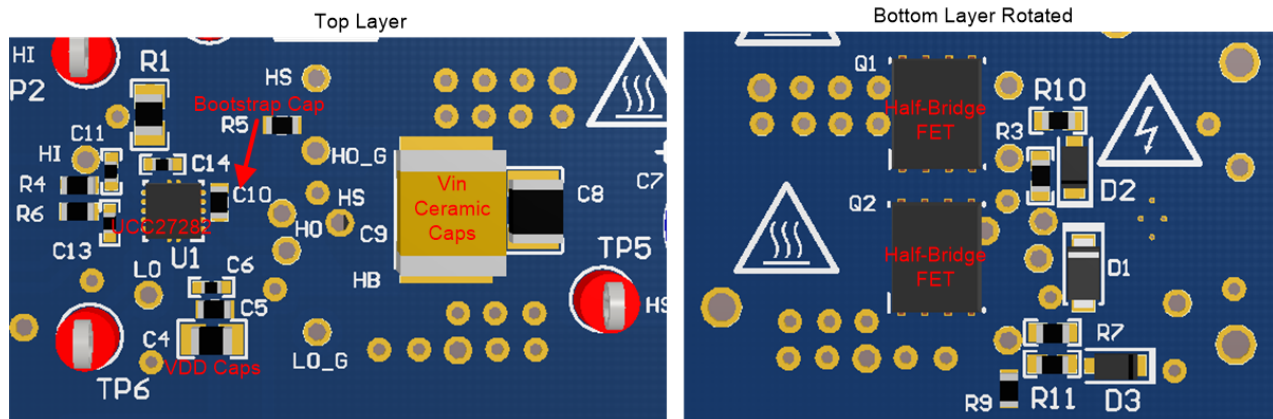
$$I_{OLL} = \frac{V_{DD}}{R_{LOL} + R_{GATE} + R_{GFET(int)}}$$

(8)

### 2.2.3 Layout Considerations

To achieve best performance the layout of the 100-V power stage requires attention to the loop inductance for both the power loop and gate drive loop. 図 2 shows a general view of the layout.

図 2. Layout General View



### 2.2.3.1 Gate Drive Loop Layout

図 3 and 図 4 show the layout of the gate loop of the upper and lower FETs. To achieve the minimum loop inductance, the layout of gate drive loop must follow these rules:

- Have the VDD capacitor or bootstrap capacitor as close as possible to the gate driver because these traces will be part of the gate loop.
- Use a dedicated Kelvin source or minimum sharing of source trace between the gate drive loop and main power loop to achieve the minimum common source inductance. The high di/dt on the power loop can easily be coupled to the gate drive loop. This may cause decreased switching speed and other negative effects.
- To keep the return loops as short as possible, vias in pads are used in this design to further reduce the parasitic inductances and improve the current extraction from components.

図 3. Gate Drive Loop Layout for High-Side FET

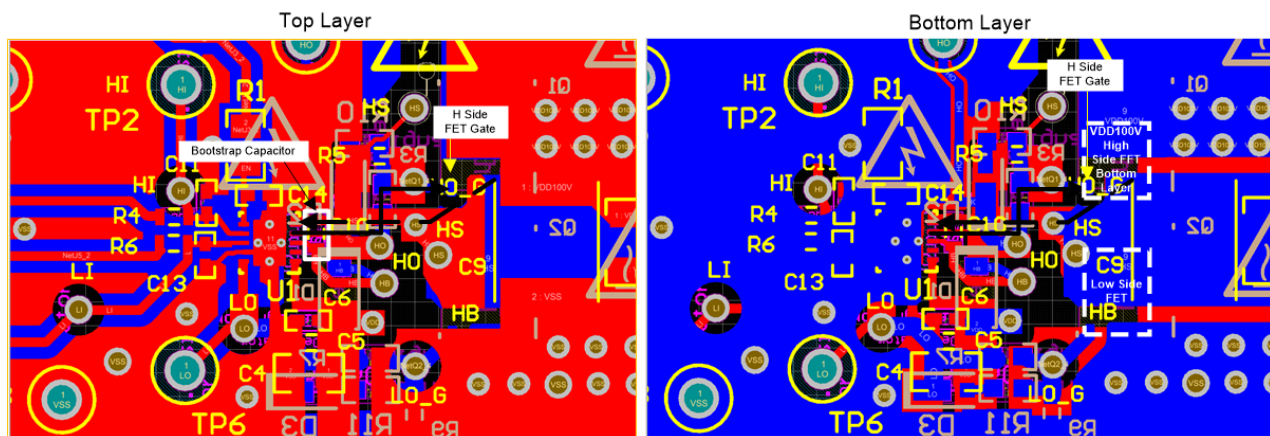
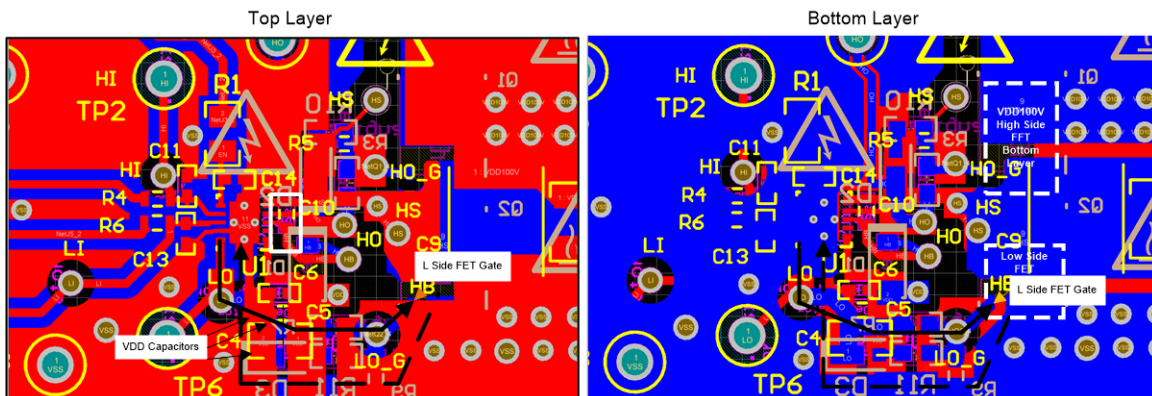




図 4. Gate Drive Loop Layout for Low-Side FET



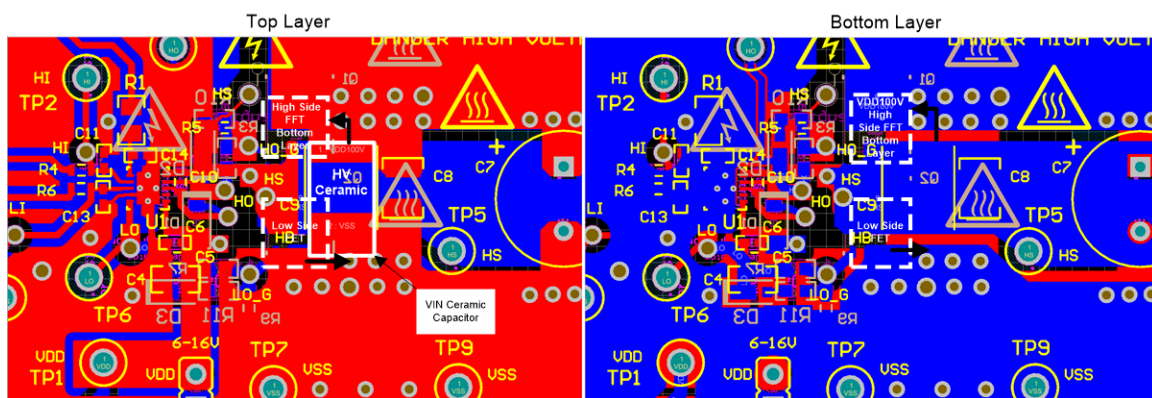
### 2.2.3.2 Power Loop Layout

The power loop layout objective is to minimize stray inductance. To realize a small power loop:

- Place ceramic capacitors with a small package as close to the devices as possible. These capacitors are usually better in frequency response and have a high bandwidth to absorb high-frequency noise generated during switching than bulk capacitors.
- A compact component placement is needed. Place the upper and lower FETs stacked from VIN to the power ground as close as possible to the input voltage ( $V_{IN}$ ) capacitors.
- Minimize the overlap between switching node and ground/Vin copper. This overlap avoids the extra parasitic capacitance, which adds to  $C_{OSS}$  of FETs. If not designed well, the parasitic capacitors can generate significant loss at high switching frequency.

図 5 shows that the size of the power loop is minimized. The ceramic capacitors are placed across VIN and ground with multiple vias connecting the other layer planes close to the FETs.

図 5. Half-Bridge Power Loop Layout



## 2.3 Highlighted Products

### 2.3.1 UCC27282

The UCC27282 is a 120-V, half-bridge, high-performance MOSFET driver designed for applications that require high drive strength, wide bias voltage operating range, low propagation delays and excellent delay matching.

The UCC27282 half-bridge driver has new features and parameter improvements to achieve optimum power module performance and enhance robustness. The wide operating VDD range of 6 V to 16 V with adequate gate drive strength enhances flexibility to optimize efficiency based on gate drive losses, resistive losses and switching loss. A low signal on the EN pin disables the driver and sets the UCC27282 in a state of low bias current  $I_{DD}$  typically 7  $\mu$ A. This low current will help achieve low standby power when the module is disabled. High-frequency operation and precise timing can be achieved due to low typical propagation delay of 16 ns and typical delay matching of 1 ns.

The UCC27282 includes an input interlock feature which prevents both gate driver outputs from being in the high state at the same time in the event both inputs are high. This will prevent cross conduction of the power MOSFETs in the case of unexpected disturbance or noise on the driver inputs. The UCC27282 operates over a wide temperature range from  $-40^{\circ}\text{C}$  to  $+140^{\circ}\text{C}$  and is offered in a small 3 x 3 QFN package.

### 2.3.2 CSD19531

The CSD19531 is a 100-V N-Channel NexFET™ designed to minimize loss in power conversion applications. The  $R_{DS(on)}$  is rated at 6.0 m $\Omega$  and 5.3 m $\Omega$  at  $V_{GS}$  of 6V and 10 V. The  $Q_G$  is only 37 nC at 10 V  $V_{GS}$  resulting in low gate drive loss.

The CSD19531 5-mm x 6-mm SON package has very low thermal resistance and is a common package size. The CSD19531 is also avalanche rated to improve the robustness of the power converter design.

The CSD19531 is well suited for power conversion applications including primary side telecom, secondary side synchronous rectification, and motor drive.



### 3 Hardware, Software, Testing Requirements, and Test Results

#### 3.1 Required Hardware

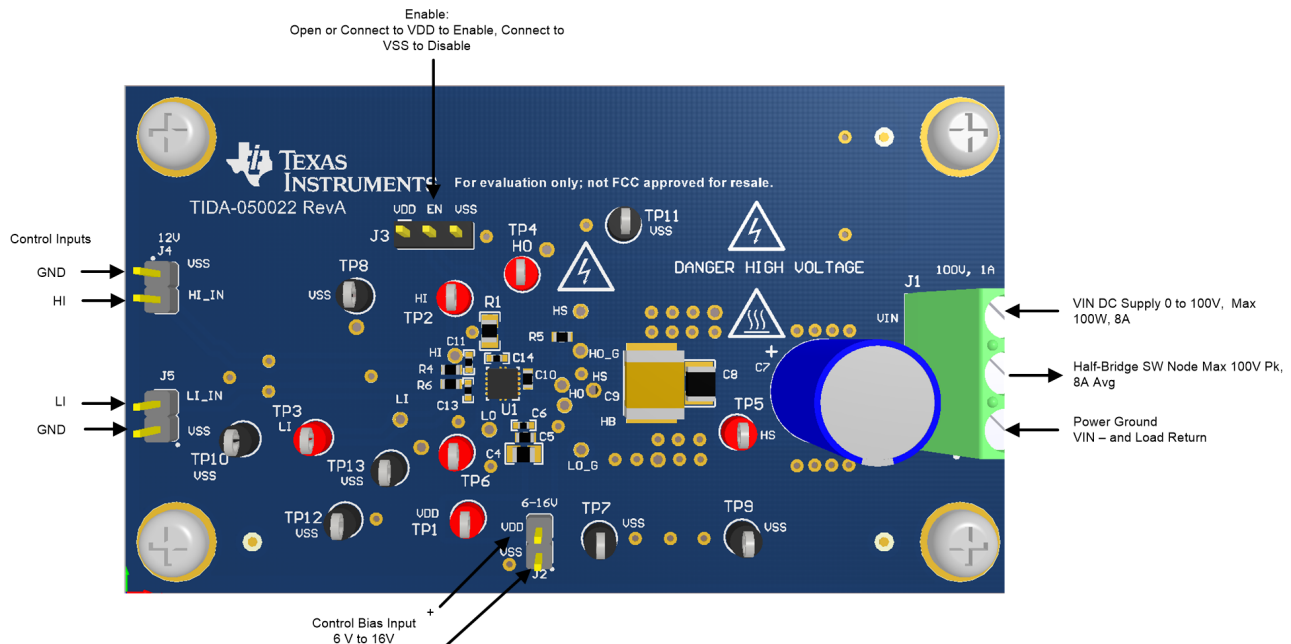
- DC voltage source: Capable of supplying the input of the board up to 100 V is desired; capable of supplying 10 A and supports current limiting
- DC bias source: Capable of 6-V to 18-V output at up to 0.3 A
- Oscilloscope: Capable of at least a 500-MHz operation, using oscilloscope probes with a "pigtail" spring ground clip instead of the standard alligator clip
- DC multimeters: Capable of 100-V measurement, suitable for determining operation and efficiency (if desired)
- DC load: Capable of 100-V operation at up to 10 A in constant current-mode operation
- Function generator
- Dual synchronous output for independent mode; capable of at least 0-V to 3-V signal.
- (Optional) Power meter: Capable of 100-V operation at up to 8 A

#### 3.2 Testing and Results

##### 3.2.1 Test Setup

Connect the input and bias supplies and DC electronic load as shown in [Figure 6](#).

**Figure 6. TIDA-050022 Top View**



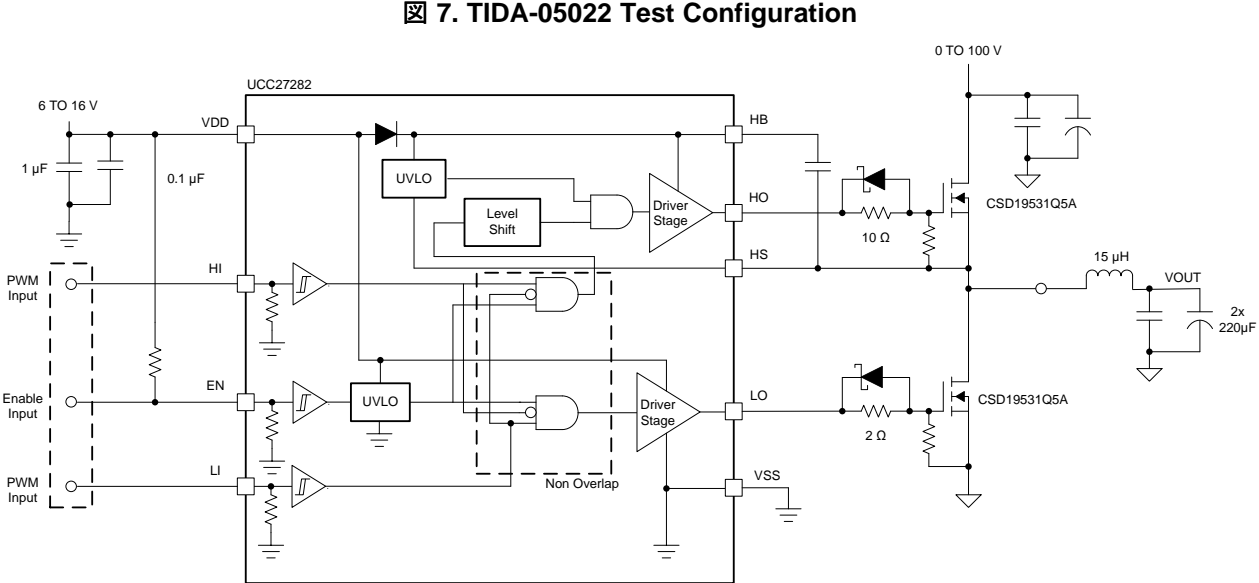
To obtain the best performance of this board:

- **Thermal:** The parts used on this board are small with limited heatsink copper. If the dissipation exceeds 4 W, actively cool the board (as it has no heat-sink) using a fan or a similar device.
- **Voltage spikes:** As the test is running, whenever increasing the voltage and the current, it is important to monitor the voltage on the switched node to ensure the peak voltage does not exceed the 100-V rating of the CSD19531 FETs as this could damage the components.

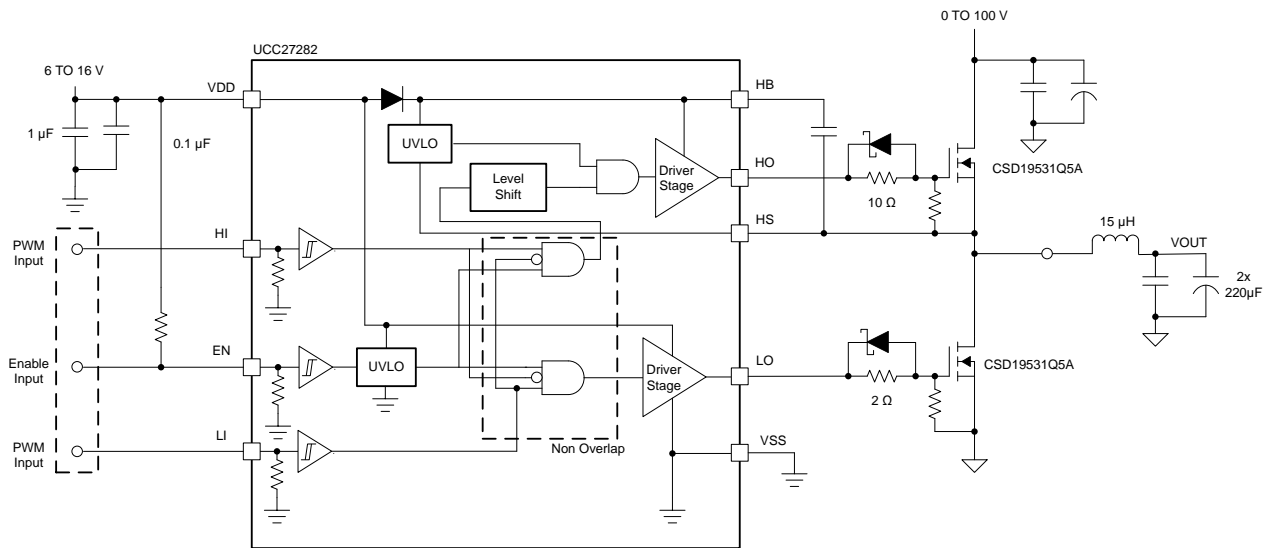
- Additional capacitance on switched nodes: Typically, the method to observe the voltage at the high-side gate and the switched node is using a voltage probe. These probes come with several tens of pF of capacitance, which given the frequency can negatively impact efficiency. For precise efficiency measurements, remove all probes connected to switching nodes.

### 3.2.2 Test Results

#### 3.2.2.1 Losses and Efficiency

The TIDA-050022 power stage is tested in a synchronous-buck configuration to illustrate optimization of converter, gate drive and total losses.  shows the tested configuration of the synchronous-buck converter operating under the following conditions:  $V_{IN} = 48\text{ V}$ ,  $f_{SW} = 200\text{ kHz}$  and  $300\text{ kHz}$ ,  $I_{OUT} = 4\text{ A(DC)}$ , LI/HI deadtime = 50 ns, 50 percent duty cycle.

**図 7. TIDA-05022 Test Configuration**



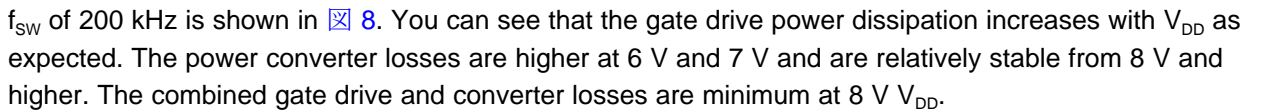
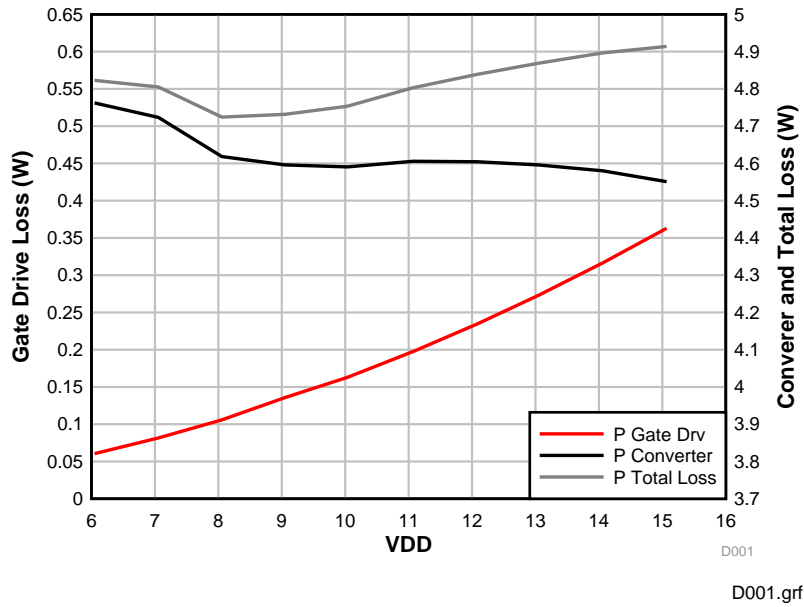
The synchronous-buck test circuit with CSD19531 MOSFETs loss data with an output power of 96 W and  $f_{SW}$  of 200 kHz is shown in . You can see that the gate drive power dissipation increases with  $V_{DD}$  as expected. The power converter losses are higher at 6 V and 7 V and are relatively stable from 8 V and higher. The combined gate drive and converter losses are minimum at 8 V  $V_{DD}$ .

図 8. Gate Drive, Converter, and Total Loss: CSD19531 MOSFETs, and  $f_{sw}$  200 kHz



In 表 2, the CSD19531 MOSFET parameters are compared to the CSD19533. Although the CSD19531 has lower  $R_{DS(on)}$ , the gate charge is higher and the body diode  $t_{RR}$  is longer than the CSD19533. Since the synchronous-buck test circuit will have continuous current operation and some body diode conduction, the body diode recovery time is an important consideration in this case. The synchronous-buck test data with the CSD19533 MOSFETs operating at 200 kHz is shown in 図 9. You can see that the minimum total losses are still with  $V_{DD} = 8V$  and the converter and total losses are lower.

In 図 10 the efficiency versus  $V_{DD}$  accounting for all losses is shown for the CSD19531 and CSD19533 MOSFETs. The CSD19533 efficiency is slightly higher in this test condition.

図 9. Gate Drive, Converter and Total Loss: CSD19533 MOSFETs, and  $f_{sw}$  200 kHz

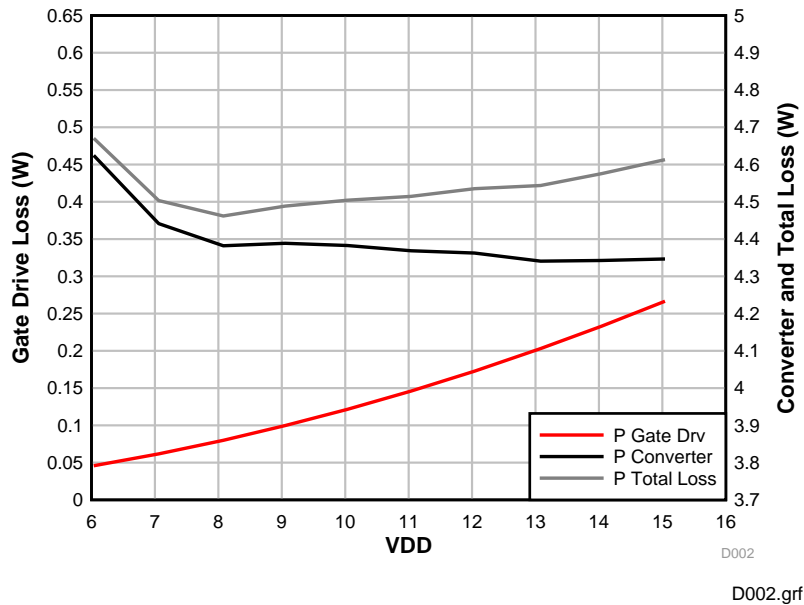
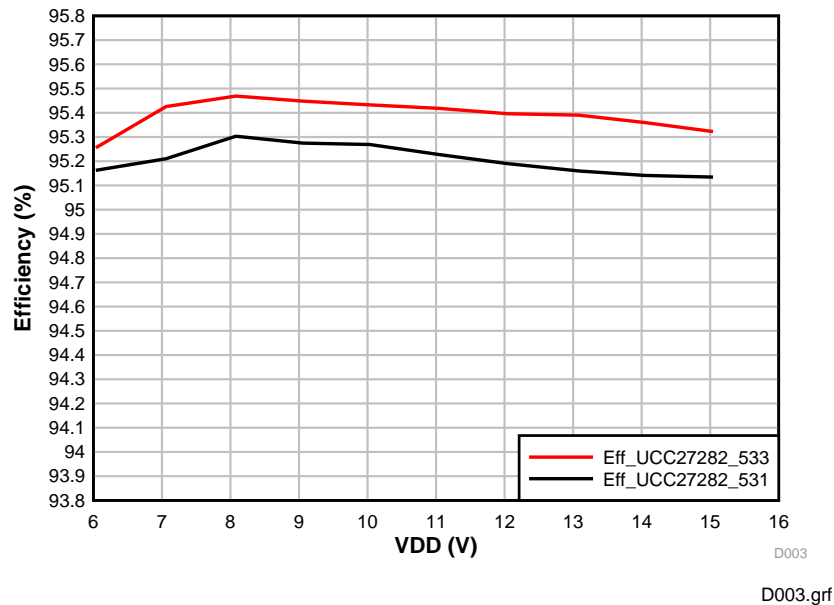


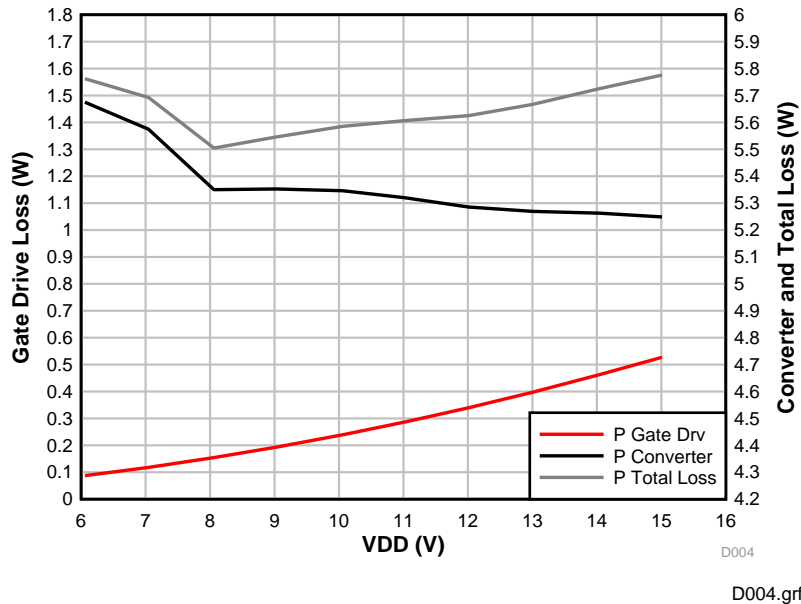
図 10. Efficiency versus  $V_{DD}$ : CSD19531 and CSD19533 MOSFETs, and  $f_{sw}$  200 kHz



The converter was also tested at a switching frequency of 300 kHz to confirm if the optimum gate drive voltage follows the same trend.

The synchronous-buck test circuit with CSD19531 MOSFETs loss data with an output power of 96 W and  $f_{sw}$  of 300 kHz is shown in [Figure 11](#). As before, the gate drive power dissipation increases with  $V_{DD}$  as expected. The power converter losses show the same trend and are higher at 6 V and 7 V and are relatively stable from 8 V and higher. The combined gate drive and converter losses are minimum at 8 V  $V_{DD}$ . Note that the overall losses are higher and the scale has increased.

**Figure 11. Gate Drive, Converter, and Total Loss: CSD19531 MOSFETs, and  $f_{sw}$  300 kHz**



With higher operating frequency the body diode recovery time will likely have more impact on the efficiency in the synchronous-buck converter. The synchronous-buck test data with the CSD19533 MOSFETs operating at 300 kHz is shown in [Figure 12](#). You can see that the minimum total losses are still with  $V_{DD} = 8V$  and the losses are considerably lower.

In [Figure 13](#), the efficiency versus  $V_{DD}$  accounting for all losses is shown for the CSD19531 and CSD19533 MOSFETs operating at 300 kHz. The CSD19533 efficiency is noticeably higher in this test condition.

図 12. Gate Drive, Converter and Total Loss: CSD19533 MOSFETs, and  $f_{sw}$  300 kHz

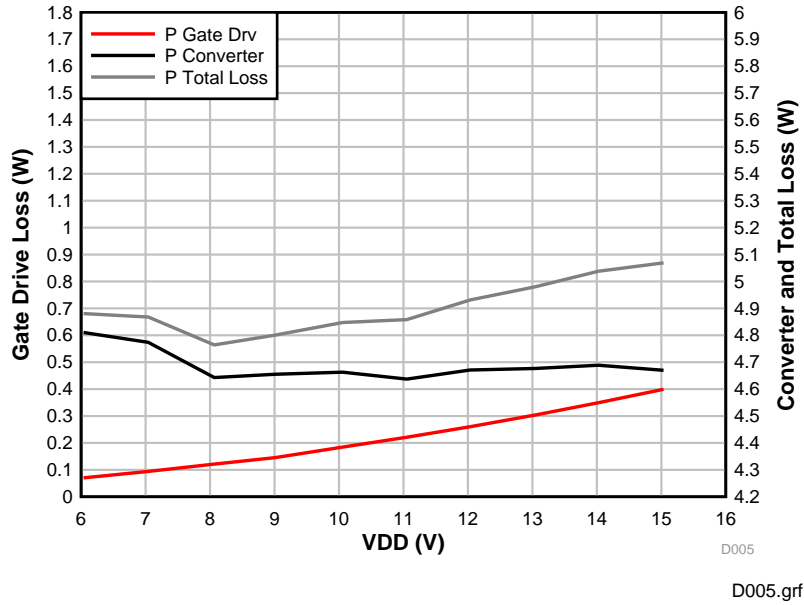
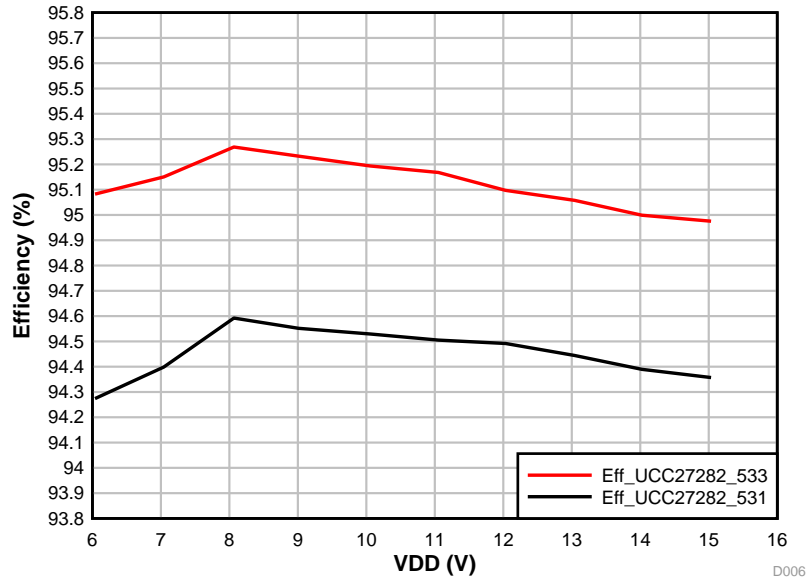


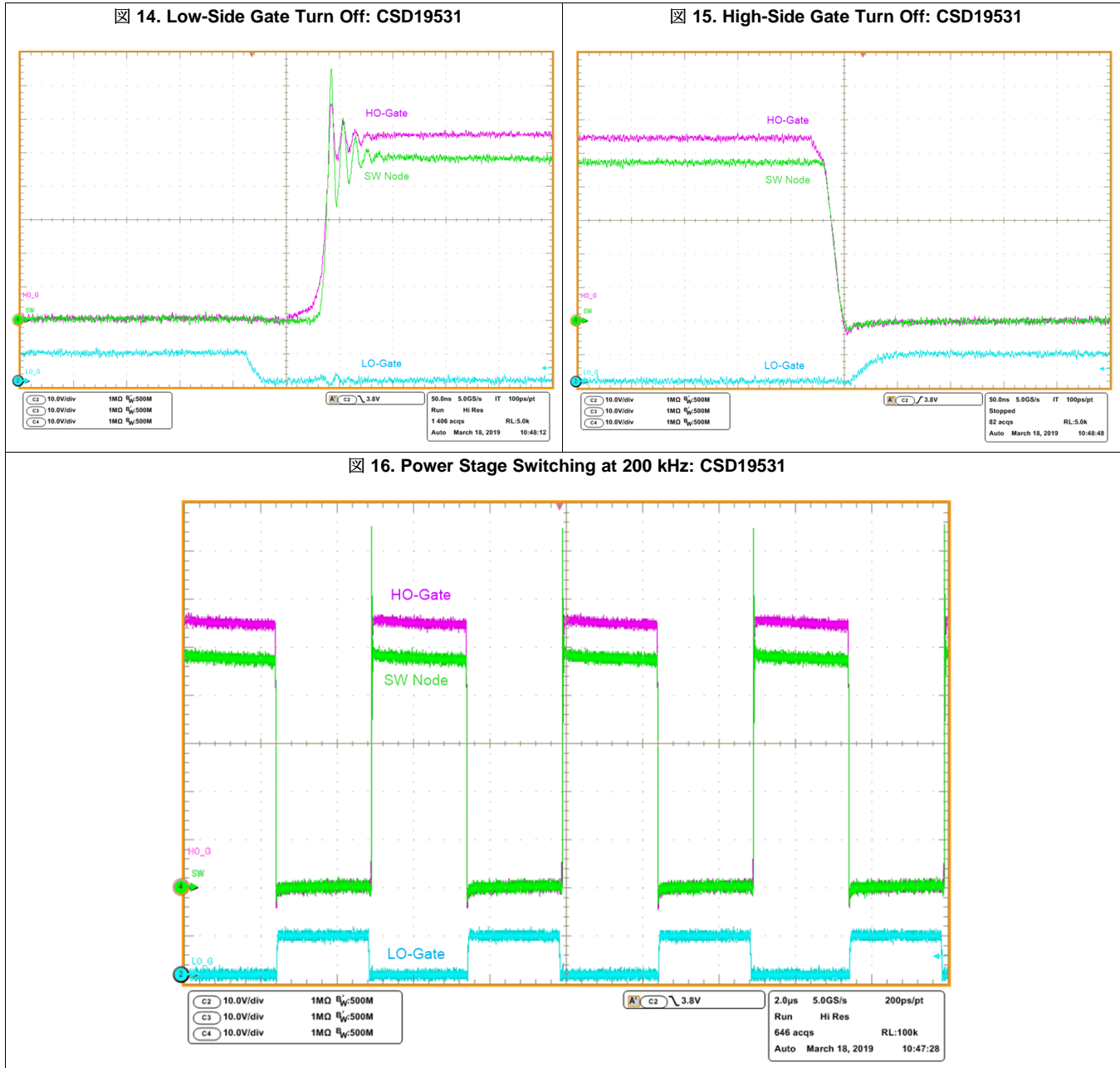


図 13. Efficiency Versus  $V_{DD}$ : CSD19531 and CSD19533 MOSFETs, and  $f_{sw}$  300 kHz



### 3.2.2.2 Switching Waveforms

Figure 14 and Figure 15 show the CDS19531 low- and high-side gate turn off waveforms. Figure 16 shows the power stage switching at 200 kHz.



## 4 Design Files

### 4.1 Schematics

To download the schematics, see the design files at [TIDA-050022](#).

### 4.2 Bill of Materials

To download the bill of materials (BOM), see the design files at [TIDA-050022](#).

### 4.3 PCB Layout Recommendations

#### 4.3.1 Layout Prints

To download the layer plots, see the design files at [TIDA-050022](#).

### 4.4 Altium Project

To download the Altium project files, see the design files at [TIDA-050022](#).

### 4.5 Gerber Files

To download the Gerber files, see the design files at [TIDA-050022](#).

### 4.6 Assembly Drawings

To download the assembly drawings, see the design files at [TIDA-050022](#).

## 5 Related Documentation

1. Texas Instruments, [Using the UCC27282EVM-335 User's Guide](#)
2. Texas Instruments, [UCC27282 120-V Half-Bridge Driver with Cross Conduction Protection and Low Switching Loss Data Sheet](#)
3. Texas Instruments, [CSD19531Q5A 100 V N-Channel Nex FET™ Power MOSFETs Data Sheet](#)

### 5.1 商標

E2E, NexFET are trademarks of Texas Instruments.

## 改訂履歴

資料番号末尾の英字は改訂を表しています。その改訂履歴は英語版に準じています。

### 2019年5月発行のものから更新

**Page**

• link 変更 .....	17
• link 変更 .....	17
• link 変更 .....	17
• link 変更 .....	17

## 重要なお知らせと免責事項

TI は、技術データと信頼性データ(データシートを含みます)、設計リソース(リファレンス・デザインを含みます)、アプリケーションや設計に関する各種アドバイス、Web ツール、安全性情報、その他のリソースを、欠陥が存在する可能性のある「現状のまま」提供しており、商品性および特定目的に対する適合性の黙示保証、第三者の知的財産権の非侵害保証を含むいかなる保証も、明示的または黙示的にかかわらず拒否します。

これらのリソースは、TI 製品を使用する設計の経験を積んだ開発者への提供を意図したものです。(1) お客様のアプリケーションに適した TI 製品の選定、(2) お客様のアプリケーションの設計、検証、試験、(3) お客様のアプリケーションに該当する各種規格や、その他のあらゆる安全性、セキュリティ、規制、または他の要件への確実な適合に関する責任を、お客様のみが単独で負うものとし、

上記の各種リソースは、予告なく変更される可能性があります。これらのリソースは、リソースで説明されている TI 製品を使用するアプリケーションの開発の目的でのみ、TI はその使用をお客様に許諾します。これらのリソースに関して、他の目的で複製することや掲載することは禁止されています。TI や第三者の知的財産権のライセンスが付与されている訳ではありません。お客様は、これらのリソースを自身で使用した結果発生するあらゆる申し立て、損害、費用、損失、責任について、TI およびその代理人を完全に補償するものとし、TI は一切の責任を拒否します。

TI の製品は、[TI の販売条件](#)、または [ti.com](https://www.ti.com) やかかる TI 製品の関連資料などのいずれかを通じて提供する適用可能な条項の下で提供されています。TI がこれらのリソースを提供することは、適用される TI の保証または他の保証の放棄の拡大や変更を意味するものではありません。

お客様がいかなる追加条項または代替条項を提案した場合でも、TI はそれらに異議を唱え、拒否します。

郵送先住所 : Texas Instruments, Post Office Box 655303, Dallas, Texas 75265

Copyright © 2022, Texas Instruments Incorporated